An analysis of Expected Population States in the Space of Population States: the Case Study of Three-Element Populations

Iwona Karcz-Duleba, Andrzej Cichon

Institute of Computer Engineering, Control and Robotics, Janiszewskiego St. 11/17, 50-372 Wroclaw, Wroclaw University of Technology, Poland
iwona.duleba@pwr.wroc.pl, andrzej.cichon@pwr.wroc.pl

Abstract: In this paper, an analysis of phenotypic evolutionary search with proportional selection and Gaussian mutation is presented. Evolution is regarded in the space of population states where population is considered as a whole. This approach enables theoretical studies of expected states for small populations. In this paper, three-element populations are examined. The expected states of populations cannot be calculated explicitly due to overwhelming complexity. Therefore, they are approximated numerically. A study of the expected states dynamics and its dependence on several parameters is also provided. It appears that the population moves around, in a fitness landscape, as a compact cluster of individuals and quickly locates neighborhoods of optima.

Keywords: evolutionary computation; small populations; space of population states; population dynamics

1 Introduction

Due to complexity, high-dimensionality and non-linearity, a theoretical study of evolutionary algorithms is rather difficult. Therefore, some simplifying assumptions have to be accepted. One of several possibilities is to consider infinite (or very large) populations [1, 2, 3]. The opposite approach is to consider populations composed of only a few individuals [4, 5]. A population can be represented in two different ways: either regarding its individuals in the space of their types, or concerning the whole population in a space of population states (a space of all possible populations). The second approach is specific for modeling evolutionary algorithms as Markov chains [6, 7] or dynamical systems [1].

In this paper, we will focus on finite, small populations evolving under proportional selection and Gaussian mutation in a real-valued space of population

states. In the real-world applications, populations are not infinite. Moreover, small populations have better exploration properties in search for the global optimum of multidimensional and multimodal quality functions. Nonetheless, using small populations in an evolutionary process has some disadvantages. Such populations behave more chaotically and are unable to maintain diversity for many generations. They cannot penetrate as large areas within a search space as more numerous ones. Also, small size of a population may lead to genetic drift which can result in reduction of a fitness value. Theoretical studies of small populations are scarce and mainly devoted to evolution strategies (ES) [8]. The presented population states approach facilitates the study of very small populations' dynamics in landscapes of one-dimensional unbounded fitness functions. These states allow us to analyze averaged (deterministic) evolution of the whole population instead of non-deterministic behavior of its elements. The expected values locate position of the averaged population and evolution may be interpreted as the population's trajectory in the space of states. Somewhat similar approaches were successfully applied to study the evolution of an ensemble of binary-coded populations in a phase space, that is a space of all possible sets of gene sequences [9], as well as to describe the averaged (macroscopic) evolutionary dynamics of simple genetic algorithm using statistical mechanics-based methods [10].

Thus far, the simplest possible case of two-element populations with one real-valued trait (gene) was studied [4, 5]. Expected values of consecutive population states were calculated and the asymptotic behavior of evolution was examined. We argue that it would be informative to extend the previous analyses to more numerous populations. Therefore, in this paper, estimation of expected values of population state for three-element populations is provided and the mean-value dynamics is evaluated.

The rest of the paper is organized as follows. In Section 2, a formal description of the considered evolution model is presented. Calculations of expected population state for three-element populations are provided in Section 3, followed by the expected dynamics studies in Section 4. Section 5 concludes this paper.

2 Model of Phenotypic Evolution

A one-dimensional version of the model of phenotypic asexual evolution, based on Darwinian theory of evolution, is regarded in the paper [11]. An *m*-element population $P=\{\boldsymbol{x}_1,\boldsymbol{x}_2,\ldots,\boldsymbol{x}_m\}$ evolves in an unbounded one dimensional (n = 1) continuous real-valued search space, so the k^{th} individual is described by one trait (*type*) $\boldsymbol{x}_k=\{x_{k,1}\}=x_k$, and corresponding quality index (*fitness*) $q(x_k)\colon \mathrm{R}\to\mathrm{R}^+$. Evolution of successive generations of individuals is ruled by two mechanisms: 1) Proportional selection (also called soft, or roulette-wheel selection) where a

parent is chosen randomly with probability proportional to its fitness, 2) Gaussian mutation producing the offspring individual by adding independent random variables, normally distributed with identical standard deviation σ to the parental traits. The model is simple but demonstrates essential properties of an evolutionary process and allows one to obtain some theoretical results for infinite [3], as well as finite (small) populations [4, 5].

Evolving populations are usually studied in a *space T of individuals' types*. In this space, when the location of i^{th} generation P^i is known, a conditional distribution of a new individual's position in the $(i+1)^{\text{st}}$ generation is given by:

$$f_T^{i+1}\left(\boldsymbol{x} \mid P^i\right) = \sum_{k=1}^{m} \alpha\left(\boldsymbol{x}_k^i\right) g\left(\boldsymbol{x}, \boldsymbol{x}_k^i\right) = \sum_{k=1}^{m} \alpha_k^i \mathrm{N}_k^i, \tag{1}$$

where $\alpha\left(\boldsymbol{x}_k^i\right) = \alpha_k^i = q\left(\boldsymbol{x}_k^i\right) \Big/ \sum_{j=1}^{m} q\left(\boldsymbol{x}_j^i\right)$ is the relative quality of the k^{th} individual, $g\left(\boldsymbol{x}, \boldsymbol{x}_k^i\right) = \mathrm{N}_k^i = \mathrm{N}\left(\boldsymbol{x}_k^i, \sigma\right)(\boldsymbol{x}) = \frac{1}{\sigma\sqrt{2\pi}} \exp\left(-\frac{\left(\boldsymbol{x} - \boldsymbol{x}_k^i\right)^2}{2\sigma^2}\right)$ describes a normal distribution of mutation, $q(\boldsymbol{x})$ denotes a non-negative fitness function, σ stands for the standard deviation of mutation.

The population as a whole is considered in *a space of population states S*. The structure of this space is seemingly more complex than the typically studied space *T*. The dimensionality of *S* depends on the population size and it is equal to $\dim S = mn$ (compared to $\dim T = n$). In the case of one-dimensional search spaces, $\dim S = m$ and $S = \mathrm{R}^m$. Additionally, as the population is insensitive to ordering of its individuals, an equivalence relation *U* has to be defined in *S* to identify all the points corresponding to permutations of individuals within the population. Consequently, the population state is reduced to a point in the quotient (factor) space $S_U = S/U = \mathrm{R}^m/U$. In this study, the relation *U* arranges individuals within population in a decreasing manner based on the values of their traits. Thus, in the case of three-element population, in the quotient space S_U the population state becomes an ordered tuple $\boldsymbol{s} = \{x_1, x_2, x_3\}$, where $x_1 \geq x_2 \geq x_3$.

When a state $\boldsymbol{s}^i$ of population in the i^{th} generation is known, the probability distribution $\tilde{f}_{S_U}^{i+1}\left(\boldsymbol{s} \mid \boldsymbol{s}^i\right)$ of the population state in S_U in the next generation can be determined. The distribution is a product of *m* individual distributions (1) considered in the space *T*:

$$\tilde{f}_{S_U}^{i+1}\left(\boldsymbol{s} \mid \boldsymbol{s}^i\right) = m! \prod_{j=1}^{m} f_T^{i+1}\left(x_j \mid \boldsymbol{s}^i\right) = m! \prod_{j=1}^{m} \sum_{k=1}^{m} \alpha\left(x_k^i\right) \mathrm{N}\left(x_k^i, \sigma\right)\left(x_j\right) = m! \prod_{j=1}^{m} \sum_{k=1}^{m} \alpha_k^i \mathrm{N}_{jk}^i. \tag{2}$$

Once the distribution (2) is defined, the expected value of next population state can be computed. Unfortunately, because of the restriction of the population state to the quotient space S_U, straightforward calculations of the expectations are only possible for two-element populations [4, 5]. For this simplest case, an expected asymptotic behavior of evolution was studied and some essential aspects of the process were discovered, namely rapid unification of initially widely diversified populations and a slow motion towards the optima of the quality function. For more numerous populations, expected values have to be approximated numerically.

3 Expected Value of Population State of Three-Element Population

Determining the expected value of the population state of a three-element population is one of the main objectives of this paper. To obtain the value, several triple definite integrals need to be calculated with integrand given in the multiplicative form of normal distribution functions with different parameters. As an illustrative example, x_1 coordinate of the expected state is given by:

$$E^{i+1}\left[x_1 \mid \boldsymbol{s}^i\right] = \int_{-\infty}^{+\infty}\int_{-\infty}^{x_1}\int_{-\infty}^{x_2} x_1 \tilde{f}_{S_U}^{i+1}\left(x_1, x_2, x_3 \mid \boldsymbol{s}^i\right) =$$

$$= \int_{-\infty}^{+\infty}\int_{-\infty}^{x_1}\int_{-\infty}^{x_2} x_1 \left(3!\prod_{j=1}^{3}\sum_{k=1}^{3}\alpha_k \mathrm{N}_{jk}\right)\mathrm{d}x_3\mathrm{d}x_2\mathrm{d}x_1 = 3!\int_{-\infty}^{+\infty}\int_{-\infty}^{x_1}\int_{-\infty}^{x_2} x_1\left(\alpha_1\mathrm{N}_{11}+\alpha_2\mathrm{N}_{12}+\alpha_3\mathrm{N}_{13}\right)\cdot$$

$$\cdot\left(\alpha_1\mathrm{N}_{21}+\alpha_2\mathrm{N}_{22}+\alpha_3\mathrm{N}_{23}\right)\cdot\left(\alpha_1\mathrm{N}_{31}+\alpha_2\mathrm{N}_{32}+\alpha_3\mathrm{N}_{33}\right)\mathrm{d}x_3\mathrm{d}x_2\mathrm{d}x_1, \qquad (3)$$

and, for simplicity, the generation number *i* was omitted within integrals. It is worth noticing that limits of integration of two inner integrals do not range from minus to plus infinity. Instead, the upper limits are constrained, since the values are calculated in a quotient space being a reduced real space (R^m / U).

Let us first denote the component integral $I_1(p,r,s)$ as:

$$I_1(p,r,s) = 3!\,\alpha_p\alpha_r\alpha_s\int_{-\infty}^{+\infty}\int_{-\infty}^{x_1}\int_{-\infty}^{x_2} x_1\,\mathrm{N}_{1p}\mathrm{N}_{2r}\mathrm{N}_{3s}\,\mathrm{d}x_3\mathrm{d}x_2\mathrm{d}x_1,$$

where *p*, *r*, *s* take values from the set {1, 2, 3} (with repetitions). In order to obtain just a single coordinate of the expected state, 27 such integrals need to be calculated. Having performed some exhaustive computations, we finally obtained the following form of I_1:

$$I_1(p,r,s)=\frac{3}{2\pi}\alpha_p\alpha_r\alpha_s\left(\frac{1}{b}\sqrt{\frac{\pi}{2}}\exp\left(-\frac{b^2\left(x_p^i-x_r^i\right)^2}{2}\right)\operatorname{erfc}\left(\frac{b\left(2x_s^i-x_p^i-x_r^i\right)}{\sqrt{6}}\right)+\right.$$

$$\left.+x_p^2\pi\left[\operatorname{erfc}\left(\frac{b\left(x_s^i-x_r^i\right)}{\sqrt{2}}\right)-\operatorname{erf}\left(\frac{b\left(x_r^i-x_p^i\right)}{\sqrt{2}}\right)-\frac{b}{\sqrt{\pi}}\,\mathrm{I}_1(p,r,s)\right]\right), \tag{4}$$

where: $\mathrm{I}_1(p,r,s)=\int_{-\infty}^{+\infty}\exp\left(-b^2\left(x_2-x_r^i\right)^2\right)\operatorname{erf}\left(b\left(x_2-x_p^i\right)\right)\operatorname{erf}\left(b\left(x_2-x_s^i\right)\right)\mathrm{d}x_2$,

$b=\left(\sqrt{2}\sigma\right)^{-1}$, and $\operatorname{erf}(x)$, $\operatorname{erfc}(x)$ are error function and complementary error function derived from normal distributions.

$\mathrm{I}_1(p,r,s)$ can only be evaluated analytically for $p = r = s$. If $p = r$ or $r = s$, the integral can be calculated using the approximation $\operatorname{erf}^2(x)\approx 1-\exp\left(-x^2\pi^2/8\right)$. For $p\neq r\neq s$, $\mathrm{I}_1(p,r,s)$ has to be computed numerically.

Ultimately, expected value of coordinate x_1 can be expressed as a sum of:

$$E^{i+1}\left[x_1\mid \boldsymbol{s}^i\right]=\sum_{p=1}^{3}\sum_{r=1}^{3}\sum_{s=1}^{3}I_1(p,r,s)\,. \tag{5}$$

Expected values of coordinates x_2 and x_3 are calculated correspondingly:

$$E^{i+1}\left[x_2\mid \boldsymbol{s}^i\right]=\sum_{p=1}^{3}\sum_{r=1}^{3}\sum_{s=1}^{3}I_2(p,r,s)\,, \tag{6}$$

$$E^{i+1}\left[x_3\mid \boldsymbol{s}^i\right]=\sum_{p=1}^{3}\sum_{r=1}^{3}\sum_{s=1}^{3}I_3(p,r,s)\,, \tag{7}$$

and their component integrals are given in Appendix 1. All calculations and simulations were performed using *Mathematica* software [12].

4 Dynamics of Expected States of Three-Element Populations

With given values of the expected states, an expected long-term behavior of the evolving three-element populations can now be analyzed. Simulations of the expected states were carried out in landscapes of different quality functions: unimodal triangle and Gaussian, both symmetrical and asymmetrical. Similarly, multi-modal functions in the form of bimodal Gaussian fitness with different

heights and various distances between optima were considered (all the functions are listed in Appendix 2). In these landscapes, population dynamics and the influence of several parameters (standard deviation of mutation σ, fitness function asymmetry, and distance between optima) was analyzed. In order to study population diversity, random and homogeneous initial populations were examined.

Expected states are a good estimation of random population behavior. In Fig. 1, locations of coordinates x_1, x_2, x_3 averaged over 50, 100 and 500 runs are presented along with expected states coordinates calculated with Eqns. (5)–(7) in the course of 30 generations. The fitness function is shown in the right panel. It can be noticed that the averaged behavior closes the expected state trajectories — the approximation accuracy is acceptable for less than 100 runs.

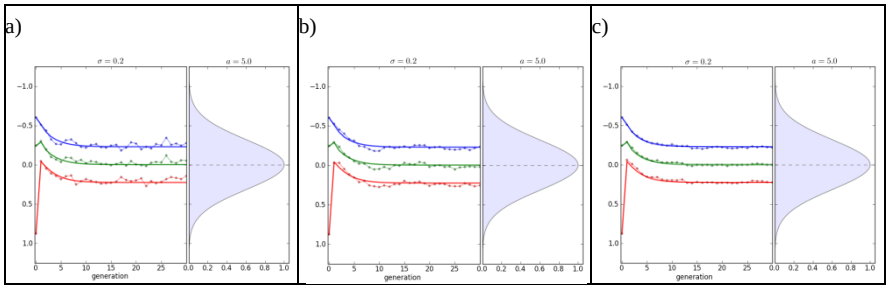

Figure 1

Random evolution of three-element populations averaged over: a) 50; b) 100; c) 500 runs (dotted lines) along with the expected states coordinates (solid lines). The red, green, and blue colors correspond respectively to coordinates x_1, x_2, x_3 of consecutive states. Parameters on the upper side of the plots specify the value of the standard deviation of mutation (σ) used in the simulations, as well as the *a* parameter of unimodal Gaussian fitness function (cf. Appendix 2)

At first, we will examine expected states trajectories in a landscape of the unimodal Gaussian fitness function with the optimum located at (0,0,0). Five trajectories of 30 generations starting from different random initial states are presented in Fig. 2 followed by Euclidean distances between consecutive states d_s in Fig. 3, and Euclidean distances between the states and the optimum d_o in Fig. 4 together with a steady state distance from optimum versus σ plot (for the distances definitions see Appendix 3).

Based on the simulations, the following observations can be made:

– At the beginning, differences in subsequent locations of trajectory points are large, thus Euclidean distances between successive states d_s are large (jumps of trajectories) (Fig. 3),

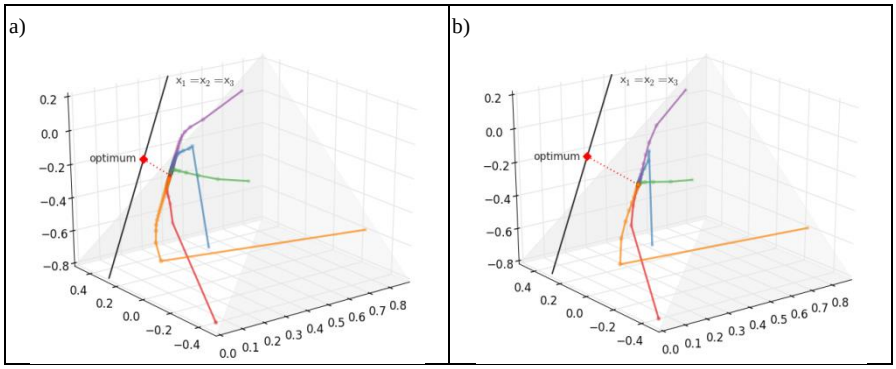

Figure 2

Five expected trajectories of three-element populations starting from different initial states. Coordinates correspond to the values of $E[x_1]$, $E[x_2]$, $E[x_3]$; identity line $x_1 = x_2 = x_3$ and the optimum are depicted. a) σ=0.1; b) σ=0.2

- Just after a few generations, the differences become much smaller, so distances d_s decrease (small steps of trajectories),
- Subsequent states are located along a line parallel to the *identity line* $x_1 = x_2 = x_3$ called *evolutionary channel* [5]; the distance between the channel and the identity line depends on σ (Fig. 2),
- Expected states do not change, i.e., trajectories starting from different initial states converge to one point (a steady state, or equilibrium point),
- The rate of convergence to the steady state depends on the standard deviation of mutation σ,
- Steady states are not located exactly at the optimum,
- Distances between subsequent states and the optimum d_o quickly decreases to a value depending on the standard deviation σ; the bigger the σ, the larger the distance to the optimum in the steady state (Fig. 4).

Trajectories of expected values of three-element populations for various unimodal fitness functions: Gaussian and triangle, in their symmetrical and asymmetrical forms are presented in Fig. 5. An influence of the standard deviation of mutation on "shift" of expected steady states from the optimum in a landscape of unimodal asymmetrical Gaussian fitness function is shown in Fig. 6.

Independently of the fitness form, initially diversified population converges rapidly (in two–three generations) and forms a cluster with a radius close to σ, as in Fig. 2, Fig. 5 d-f, and Fig. 7 d-f. When the initial population is homogeneous, it becomes instantly diversified by the mutation operator and, in the following generations, forms the cluster as well (Fig. 5 a-c), (Fig. 6), (Fig. 7 a-c), (Fig. 8 a).

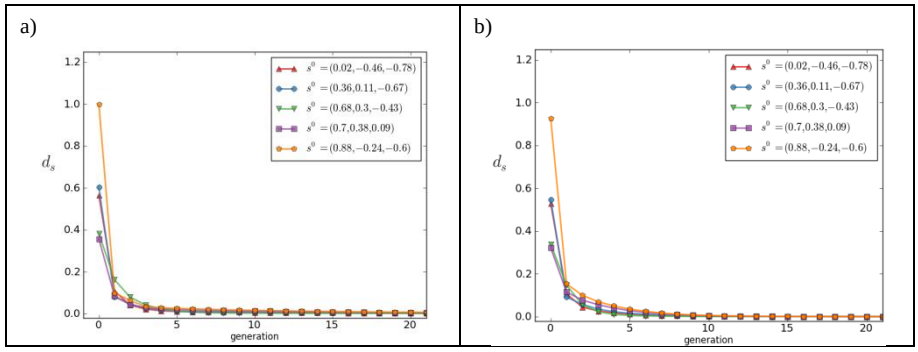

Figure 3

Distances between successive states d_s for five trajectories starting from different initial states given in Fig. 2. a) σ=0.1; b) σ=0.2

In the case of an initially homogeneous population, $x_1^0 = x_2^0 = x_3^0 = x^0$, thus $q(x_1^0) = q(x_2^0) = q(x_3^0)$, and it is possible to calculate directly on the expected values using (5)–(7):

$$E^1\left[x_1 \mid \boldsymbol{s}^0\right] \approx x^0 + 0.85\sigma, \tag{8}$$

$$E^1\left[x_2 \mid \boldsymbol{s}^0\right] \approx x^0, \tag{9}$$

$$E^1\left[x_3 \mid \boldsymbol{s}^0\right] \approx x^0 - 0.85\sigma. \tag{10}$$

Coordinate x_2 remains unchanged, while the other two differ from their initial positions by about σ — a homogeneous population is spread out by the operation of mutation. The case will be also discussed later on.

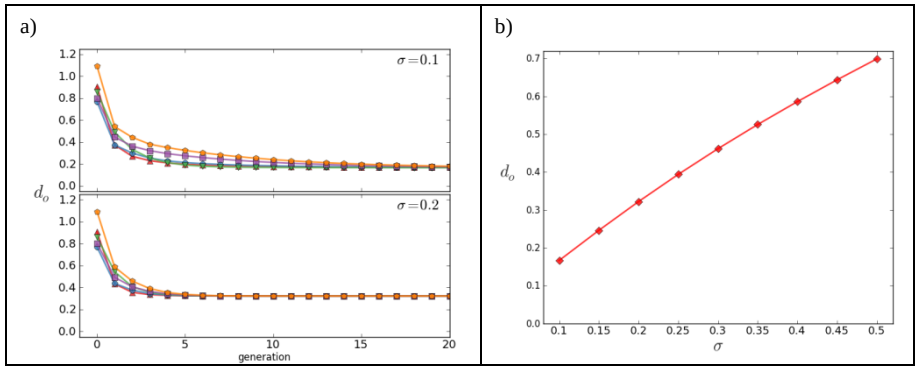

Figure 4

a) Distances between successive states and the optimum d_o for five trajectories starting from different initial populations plotted in Fig. 2 and specified in Fig. 3, for σ=0.1 and σ=0.2.

b) A steady state distance from the optimum d_o versus σ

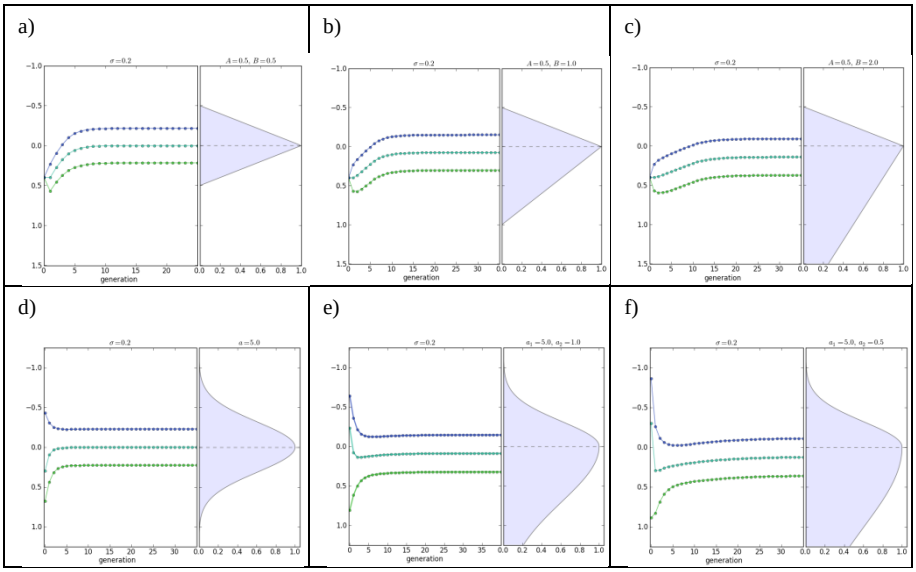

Figure 5

Evolution of expected values of three-element populations in the landscapes of unimodal symmetrical (a, d) and asymmetrical (b, c, e, f) fitness functions: a)-c) triangle; d)-f) Gaussian; σ=0.2

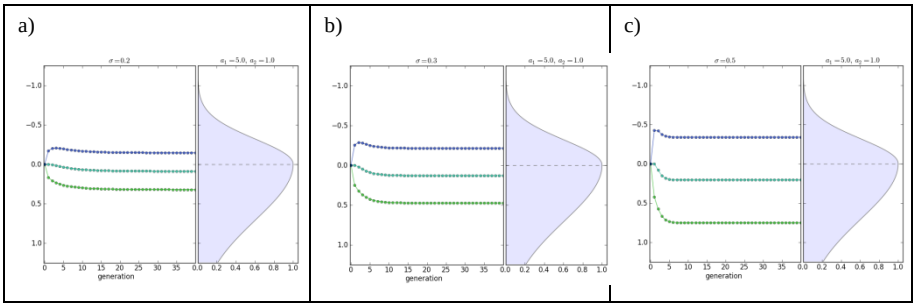

Figure 6

Influence of standard deviation of mutation on "shift" of expected steady states in a landscape of unimodal asymmetrical Gaussian fitness function: a) σ=0.2; b) σ=0.3; c) σ=0.5

When unimodal fitness function is symmetrical, $E\left[x_1 \mid \boldsymbol{s}^i\right]$ and $E\left[x_3 \mid \boldsymbol{s}^i\right]$ are situated symmetrically on the slopes of the function in equal distances from the optimum, while $E\left[x_2 \mid \boldsymbol{s}^i\right]$ is located at the optimum (which is good news for the optimum seekers) (Fig. 5 a, d). Asymmetry in the fitness landscape affects the expected states: they are shifted towards the slope with a "bigger mass": the greater the asymmetry, the greater the displacement (Fig. 5 b, c, e, f). Moreover, the magnitude of the shift depends on σ: the attraction strength increases along with the value of σ (Fig. 6).

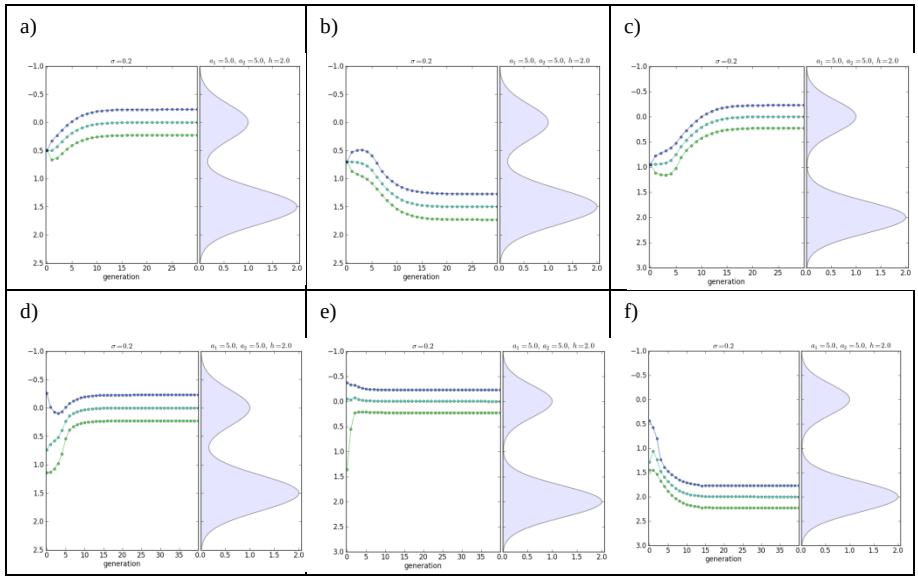

Figure 7

Evolution of expected values of three-element populations in a landscape of bimodal Gaussian fitness functions. Homogenous initial population (a-c) lies in a basin of attraction of the local (a, c) and the global (b) optimum. Random initial population (d-f) in a basin of attraction of the local (d, e) and the global (f) optimum. Functions represent different distances between optima: a), b), d) d=1.5; c), e), f) d=2; σ=0.2

Now, let us discuss the case of bimodal fitness functions. The considered functions have got two basins of attraction corresponding to the local and the global optimum. Evolution of expected values of three-element populations in a landscape of bimodal Gaussian fitness functions with different distances between optima d for homogenous and random initial populations are shown in Fig. 7. Expected states trajectories for uniformly distributed initial states are presented in Fig. 8a, followed by Euclidean distances between successive states and the optimum in Fig. 8b.

The expected population converges to the vicinity of one of the optima and its trajectory depends both on the initial population state and σ. As to the evolution of expected states over unimodal fitness landscape (cf. Fig. 2), additional observations for homogeneous initial state can be noted:

- Immediately, in the first generation, population is diversified and its expected state is pushed away from the identity line (jumps of trajectories),
- Subsequent states are located along the evolutionary channel; the channel is more distinct than in the case of initially diversified population (Fig. 2),

- Distances between consecutive states in the channel are small and converge to zero,
- Trajectories converge to the local/global optimum when starting within a basin of attraction of the local/global optimum (Fig. 7 a-c), (Fig. 8a),
- Distances between subsequent states and the optimum decrease rapidly (Fig. 8b),
- Distances of steady states from related optimum are the same for local and global ones.

A border between basins of attraction of both optima, displayed in Fig. 9, is situated on the saddle and its accurate position depends on a distance between optima *d* and on the standard deviation of mutation σ. With the increasing value of σ, the strength of the global optimum attraction intensifies: a population is more dispersed and more easily attracted. The initially diversified population (Fig. 7 d-f) may converge to local or global optimum in the initial-state-dependent manner.

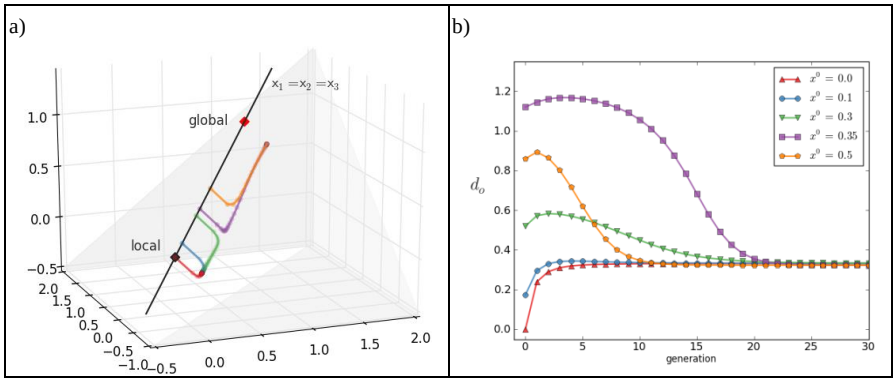

Figure 8

a) Trajectories of expected values of three-element populations starting from different homogeneous initial states in a landscape of bimodal fitness function. b) Distances between successive states and the optimum d_o for five trajectories given in the left panel. Two upper lines (for $x^0 = 0.35$, and $x^0 = 0.5$) correspond to trajectories attracted by the global optimum, three lower ($x^0 = 0.0$, $x^0 = 0.1$, $x^0 = 0.3$) correspond to trajectories attracted by the local optimum; σ=0.2

Analogously to unimodal fitness functions, the expected population in the steady state forms a cluster in the vicinity of the optimum. However, expected coordinate $E\left[x_2 \mid \boldsymbol{s}^i\right]$ is not located exactly at the optimum any more but it is moved by the influence of the other hill. The shift of population's steady state from the optimum is presented in Fig. 10. A value of the shift is a function of the distance between optima *d* and the standard deviation of mutation. Clearly, the global optimum attracts populations much stronger than the local one, and consequently the shift on the local hill towards the global one is much bigger than the other way around.

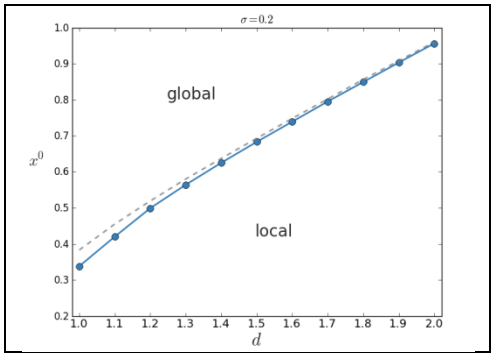

Figure 9

Border between basins of attraction of the global and the local optimum as a function of distance between optima *d*. Dotted line indicates saddle minimum. Homogeneous initial population, σ=0.2.

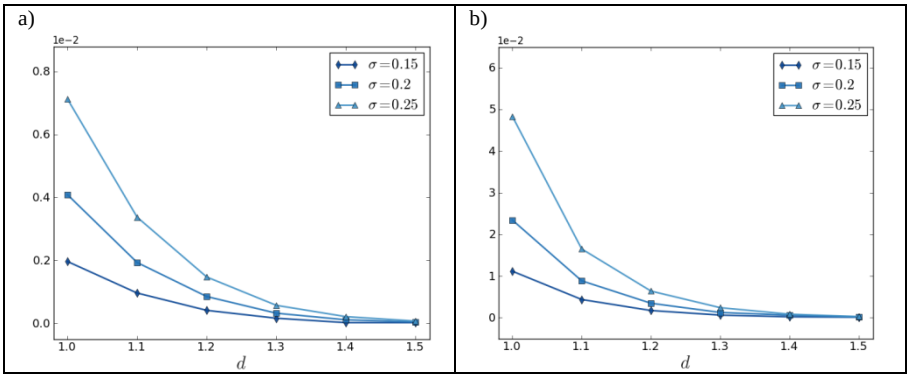

Figure 10

Shift of population's steady state from the optimum versus distance between optima *d* for: a) the global optimum; b) the local optimum

5 Summary

The work presented herein for expected states of three-element populations, facilitates understanding of the rules of artificial evolution, hence, may be useful in improving efficiency of evolutionary algorithms. The following conclusions are justified:

- Initially diversified (random) populations quickly converges to a cluster with a radius close to σ. Thus, efforts of many practitioners to widely diversify initial populations, in order to avoid premature convergence, may be abortive,

- Initially homogenous populations quickly disperse to a cluster with a radius close to σ,
- Expected states of populations in the cluster slowly move along the evolutionary channel and converge to a steady state near the optimum,
- Although the steady state is placed at some distance from the optimum, expected values of second coordinate $E\left[x_2 \mid \boldsymbol{s}^i \right]$ locate the optimum for symmetrical fitness functions. This distance depends on the standard deviation of mutation, σ, and the fitness function,
- The shift of expected population from the optimum may indicate bigger mass in the shift direction, i.e., asymmetry of unimodal function or a saddle in multi-modal landscape. These observations may be useful for identification of black-box or grey-box fitness functions.

The examined behavior of three-element populations is qualitatively very similar to that of two-element systems [4, 5], thus we presume that obtained results can be extended for more numerous (but still small) populations. Preliminary simulations of evolution of more numerous populations in the quotient space of population states revealed that properties discussed herein are accurate. In the future, more dimensional type spaces should be examined using the population space paradigm. Simulations of a conventional evolution in more dimensional types spaces T ($n > 1$) confirmed a similar population behavior: unification of diversified population, progress along evolutionary channel and fluctuation in a neighborhood of the optimum. In more numerous populations and in multidimensional spaces, no analytical formulas for expected values exist (as in the simplified models). Presumably, numerical simulations will become more cumbersome, as integrals needed to obtain the expected values, are more complex.

Appendix 1: Component integrals for coordinates x_2 and x_3

Component integrals for $E^{i+1}\left[x_2 \mid \boldsymbol{s}^i \right]$ and $E^{i+1}\left[x_3 \mid \boldsymbol{s}^i \right]$ are given by:

$$I_2\left(p,r,s\right) = \frac{3}{2\pi}\alpha_p\alpha_r\alpha_s\left(\frac{1}{b}\sqrt{\frac{\pi}{2}}\left[\exp\left(-\frac{b^2\left(x_r^i - x_s^i\right)^2}{2}\right) - \exp\left(-\frac{b^2\left(x_r^i - x_p^i\right)^2}{2}\right)\right] + \right.$$

$$\left. + x_r^i\pi\left[\operatorname{erfc}\left(\frac{b\left(x_s^i - x_r^i\right)}{\sqrt{2}}\right) - \operatorname{erf}\left(\frac{b\left(x_r^i - x_p^i\right)}{\sqrt{2}}\right) - b\sqrt{\pi}\,\mathrm{I}_2\left(p,r,s\right)\right]\right.$$

$$I_3(p,r,s)=\frac{3}{2\pi}\alpha_p\alpha_r\alpha_s\left(-\frac{1}{b}\sqrt{\frac{\pi}{2}}\exp\left(-\frac{b^2\left(x_r^i-x_s^i\right)^2}{2}\right)\operatorname{erfc}\left(\frac{b\left(x_r^i+x_s^i-2x_p^i\right)}{\sqrt{6}}\right)+\right.$$

$$\left.+x_s^2\pi\left[\operatorname{erfc}\left(\frac{b\left(x_s^i-x_r^i\right)}{\sqrt{2}}\right)-\operatorname{erf}\left(\frac{b\left(x_r^i-x_p^i\right)}{\sqrt{2}}\right)-\frac{b}{\sqrt{\pi}}\,\mathrm{I}_3(p,r,s)\right]\right)$$

where:

$$\mathrm{I}_2(p,r,s)=\int_{-\infty}^{+\infty}x_2\exp\left(-b^2\left(x_2-x_r^i\right)^2\right)\operatorname{erf}\left(b\left(x_2-x_p^i\right)\right)\operatorname{erf}\left(b\left(x_2-x_s^i\right)\right)\mathrm{d}x_2,$$

$$\mathrm{I}_3(p,r,s)=\int_{-\infty}^{+\infty}\exp\left(-b^2\left(x_2-x_r^i\right)^2\right)\operatorname{erf}\left(b\left(x_2-x_p^i\right)\right)\operatorname{erf}\left(b\left(x_2-x_s^i\right)\right)\mathrm{d}x_2,$$

and $b=\left(\sqrt{2}\sigma\right)^{-1}$.

Appendix 2: Fitness functions

Triangle fitness function with parameters *A*, *B*

$$f(x)=\begin{cases}x/A+1 & \text{for } x\in[-A,0),\ A>0\\ -x/B+1 & \text{for } x\in[0,B),\ B\geq A\\ 0 & \text{otherwise}\end{cases}.$$

Unimodal Gaussian fitness function parameterized with *A* and *B*

$$f(x)=\begin{cases}\exp(-Ax^2) & \text{for } x\leq 0\\ \exp(-Bx^2) & \text{for } x>0\end{cases},$$

for a symmetric version: $f(x)=\exp(-ax^2)$.

Bimodal Gaussian fitness function composed of two unimodal hills with different heights (*h*) and distance between optima *d*

$$f(x)=\exp(-a_1x^2)+h\exp(-a_2(x-d)^2).$$

Appendix 3: Definitions of Euclidean distances d_s and d_o

The values of distances between consecutive states d_s, and between consecutive states and the optimum d_o are calculated as Euclidean metrics. For the given coordinates of successive states $\boldsymbol{s}^0$, $\boldsymbol{s}^1$, $\boldsymbol{s}^2$,…, $\boldsymbol{s}^i$ in m-dimensional space S_U, the optimum $\boldsymbol{x}^*$, and the number of generations i, we get:

$$d_s^k\left(\boldsymbol{s}^k,\ \boldsymbol{s}^{k+1}\right)=\left\|\boldsymbol{s}^k-\boldsymbol{s}^{k+1}\right\|=\left(\sum_{j=1}^{m}\left(s_j^k-s_j^{k+1}\right)^2\right)^{1/2},\ \text{for}\ k=0,\ldots,i-1,$$

and

$$d_o^k\left(\boldsymbol{s}^k,\ \boldsymbol{x}^*\right)=\left\|\boldsymbol{s}^k-\boldsymbol{x}^*\right\|=\left(\sum_{j=1}^{m}\left(s_j^k-x_j^*\right)^2\right)^{1/2},\ \text{for}\ k=0,\ldots,i.$$

References

[1] M. D. Vose. The Simple Genetic Algorithm. Foundations and Theory. MIT Press, 1999

[2] S. Voget. Theoretical Analysis of GA with Infinite Population Size. Complex Systems, 10(3), 1996, pp. 167-183

[3] I. Karcz-Duleba. Dynamics of Infinite Populations Evolving in a Landscape of Uni- and Bimodal Fitness Functions. IEEE Transactions on Evolutionary Computations, 5(4), 2001, pp. 398-409

[4] I. Karcz-Duleba. Asymptotic Behavior of Discrete Dynamical System Generated by Simple Evolutionary Process. Journal of Applied Mathematics and Computer Science, 14(1), 2004, pp. 79-90

[5] I. Karcz-Duleba. Dynamics of Two-Element Populations in the Space of Population States. IEEE Transactions on Evolutionary Computations, 10(2) 2006, pp. 199-209

[6] A. E. Nix, M. D. Vose. Modeling Genetic Algorithms with Markov Chains. Annals of Mathematics and Artificial Intelligence, 5, 1992, pp. 79-88

[7] T. E. Davis, J. C. Principe. A Markov Chain Framework for the Simple Genetic Algorithm. Evolutionary Computation, 1(3), 1993, pp. 269-288

[8] H.-G. Beyer. The theory of evolution strategies. Berlin, Springer-Verlag, 2001

[9] A. Prügel-Bennett. Modelling Evolving Populations. Journal of Theoretical Biology, 185(1), 1997, pp. 81-95

[10] J. L. Shapiro. Statistical Mechanics Theory of Genetic Algorithms. Theoretical Aspects of Evolutionary Computing, 2001, pp. 87-108

[11] R. Galar. Evolutionary Search with Soft Selection. Biological Cybernetics, 60, 1989, pp. 357-364

[12] A. Cichon. Expected State of Three-Element Populations. (in Polish) Technical Report of Institute of Computer Engineering, Control and Robotics, No. 21, 2013. English excerpt of the report and *Mathematica* source code are available at http://iwona.duleba.staff.iiar.pwr.wroc.pl/-Acta_files/index.html